A TEST OF MULTIPLE IONIZATION SCALING IN Sc

by

Joal J. Newcomb

B.S., Southwestern Oklahoma State University, 1976

A MASTER'S THESIS

submitted in partial fulfillment of the

requirements for the degree

MASTER OF SCIENCE

Department of Physics

KANSAS STATE UNIVERSITY
Manhattan, Kansas

1979

Approved by:

Patrick Richard
Major Professor

TABLE OF CONTENTS

	Page
LIST OF TABLES	ii
LIST OF FIGURES	iii
ACKNOWLEDGEMENT	iv
I. INTRODUCTION	1
II. EXPERIMENTAL TECHNIQUE	17
III. DISCUSSION	25
IV. CONCLUSION	43
REFERENCES	50
APPENDIX	54
ABSTRACT	

LIST OF TABLES

		Page
Table I	Scandium Relative Satellite Intensities	52
Table II	Binding Energy Correction Factors for Sc	53

LIST OF FIGURES

		Page
Fig. 1	X-ray Spectrum of H + Sc	4
Fig. 2	X-ray Spectrum of C + Sc	6
Fig. 3	X-ray Spectrum of N + Sc	8
Fig. 4	X-ray Spectrum of O + Sc	10
Fig. 5	X-ray Spectrum of F + Sc	12
Fig. 6	X-ray Spectrum of Cl + Sc	14
Fig. 7	Reflective Focusing by the Johansson Method	19
Fig. 8	Target Chamber	22
Fig. 9	Block Diagram of Electronics	24
Fig. 10	$\langle \ell \rangle$ Versus V for Sc KL^n Satellite Data	27
Fig. 11	$\langle \ell \rangle / Z_1^2$ Versus V for Sc KL^n Satellite Data	29
Fig. 12	Sc Data Scaled from Ar	32
Fig. 13	PWBA Scaling	35
Fig. 14	BEA Scaling	37
Fig. 15	SCA Function	40
Fig. 16	Low Z_1 Scaling	42
Fig. 17	$\langle r \rangle$ for Projectile and Target	46
Fig. 18	Target Scaling	49

ACKNOWLEDGMENTS

I would like to thank my major professor, Pat Richard, for his guidance, his encouragement, and especially, his indispensible help in all phases of this thesis.

I would like to thank my wife, Peggy, for her love and support and also, for her efforts in typing this thesis.

I would also like to thank Jim McGuire for the private discussions which greatly aided in the development of this thesis.

I am indebted to my co-workers, Keith Jamison, Carl Schmiedekamp, Jim Hall and Phil Fepmiller for their aid and cooperation in this experiment.

I would also like to acknowledge the financial support of the Division of Chemical Sciences, U. S. Department of Energy.

I. INTRODUCTION

In recent years, many studies of single K-shell, multiple L-shell ionization formed in ion-atom collisions have been performed.[1-4] The observed statistical distribution of the Kα satellites has been explained in terms of the probabilities for simultaneous K-shell and L-shell ionization.[5,6] The probabilities for the L-shell ionization have been treated as a fitting parameter in calculating the single K-shell, multiple L-shell x-ray spectra. The systematics of these parameters have not agreed with the predictions of ionization theories, particularly, as the projectile charge, Z_1, approaches the target charge, Z_2.[7-10]

In two very recent studies of single K-shell, multiple L-shell ionization, "universal" scaling laws have been proposed by Schmiedekamp et al.[11] and Watson et al.[12] In the previous work by Schmiedekamp et al.,[11] a "universal" scaling of the average number of L-shell vacancies, $<\ell>$, was obtained for argon Kα x-ray satellites formed in H, C, N, O, F, Si, and Cl bombardment in the energy range of 1 - 5 MeV/amu. Watson et al.[12] used beams of He, C, O, and Ne incident on targets of Al, Si, and Cl as a basis for a semiempirical representation of the average L-shell ionization probability, $\bar{P}_L$, in terms of a "universal" velocity function.

The purpose of the present work was to extend these studies to higher target and projectile Z and to examine these "universal" scaling laws in the realm of higher target and projectile Z. The scaling law proposed by Schmiedekamp et al.[11] was based on spectra obtained from a gas target. In the present work, the scaling law was examined for a solid target having a Z near that of argon.

In this study, a thick scandium slab was used as the target. Figures 1 - 6 show scandium Kα x-ray satellite spectra for incident projectiles of H, C, N, O, and Cl at 1.50 MeV/amu and F at 1.75 MeV/amu. These spectra are representative of multiple ionization spectra. From spectra such as these, the average number of L-shell vacancies, $<\ell>$, can be calculated using the definition

$$<\ell> \equiv \frac{\sum_n (I_n/\omega_n)}{\sum_n (I_n/\omega_n)}$$

where n is defined as the number of L-shell vacancies giving rise to the particular satellite, I_n is the intensity of the n^{th} satellite, and ω_n is the fluorescence yield of the n^{th} satellite transition.

If the vacancy production follows binomial statistics, the average number of L-shell vacancies can be expressed in terms of the probability of L-shell ionization at zero impact parameter, $P_L(0)$, by

$$<\ell> = 8P_L(0).$$

If effects of vacancy rearrangement, vacancy dependent K-fluorescence yields, and vacancy production by electron transfer are small, then

$$8P_L(0) = \frac{\sum_n nI_n}{\sum_n I_n},$$

which leads to the experimental definition of $<\ell>$,

$$<\ell> = \frac{\sum_n nI_n}{\sum_n I_n}.$$

It was this experimental definition, shown by Schmiedekamp et al.[11] to be a good approximation, that was used throughout this thesis.

Figure 1: Scandium Kα x-ray spectrum resulting from bombardment by 1.50 MeV/amu H^+. The open circles represent data points and the solid line represents a least squares fit of the spectrum.

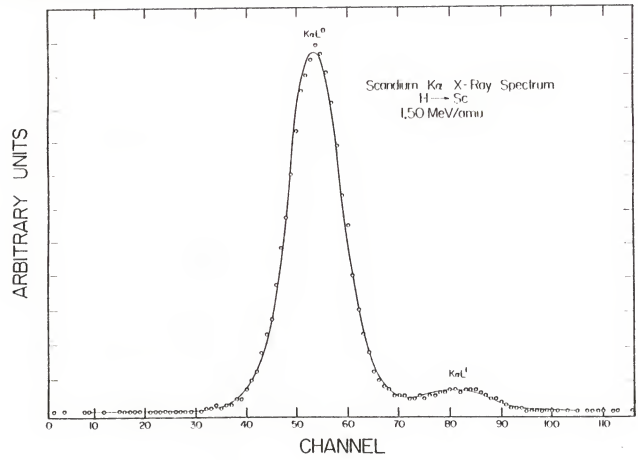
Scandium Kα X-Ray Spectrum
H → Sc
1.50 MeV/amu
KαL⁰
KαL¹
ARBITRARY UNITS
CHANNEL
0
10
20
30
40
50
60
70
80
90
100
110

Figure 2: Scandium Kα x-ray spectrum resulting from bombardment by 1.50 MeV/amu C ions. The open circles represent data points and the solid line represents a least squares fit of the spectrum.

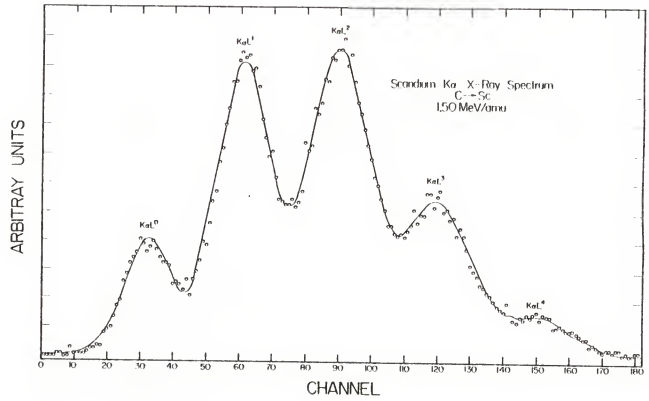
Scandium Kα X-Ray Spectrum
C--Sc
1.50 MeV/amu
Kα1,2
Kα1
Kα0
Kα3
Kα4
ARBITRAY UNITS
CHANNEL
0
10
20
30
40
50
60
70
80
90
100
110
120
130
140
150
160
170
180

Figure 3: Scandium Kα x-ray spectrum resulting from bombardment by 1.50 MeV/amu N ions. The open circles represent data points and the solid line represents a least square fit of the spectrum.

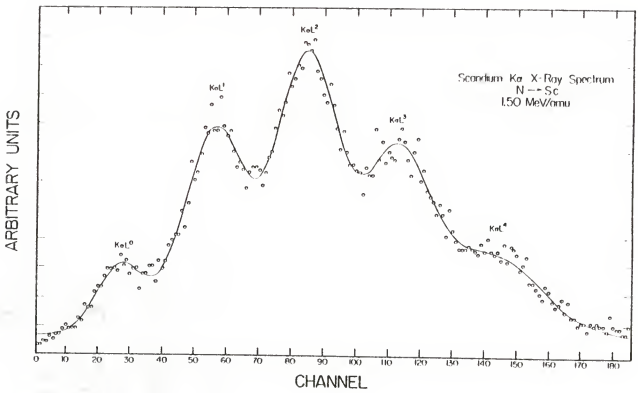
Scandium Kα X-Ray Spectrum
N – Sc
150 MeV/amu
Kα1⁰
Kα1¹
Kα1²
Kα1³
Kα1⁴
ARBITRARY UNITS
0 10 20 30 40 50 60 70 80 90 100 110 120 130 140 150 160 170 180
CHANNEL

Figure 4: Scandium Kα x-ray spectrum resulting from bombardment by 1.50 MeV/amu O ions. The open circles represent data points and the solid line represents a least squared fit of the spectrum.

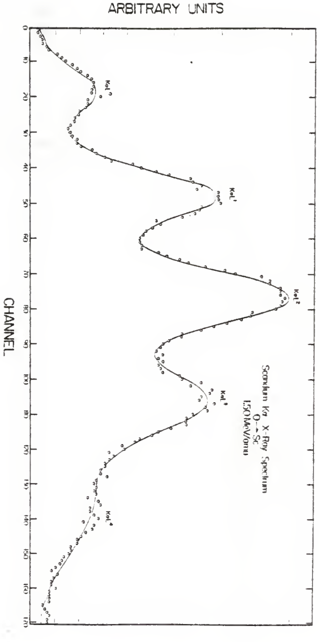
ARBITRARY UNITS
CHANNEL
Scandium Kα X-Ray Spectrum
O → Sc
1.50 MeV/amu

Figure 5: Scandium Kα x-ray spectrum resulting from bombardment by 1.75 MeV/amu F ions. The open circles represent data points and the solid line represents a least squares fit of the spectrum.

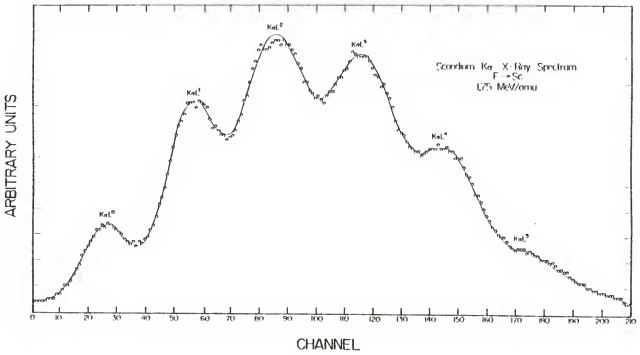
Scandium $K\alpha_{1,2}$ X-Ray Spectrum
Z = 21
1.75 MeV/emu
Kα1,2
Kα1
Kα2
Kα3
Kα4
Kα5
ARBITRARY UNITS
0 10 20 30 40 50 60 70 80 90 100 110 120 130 140 150 160 170 180 190 200 210
CHANNEL

Figure 6: Scandium Kα x-ray spectrum resulting from bombardment by 1.50 MeV/amu Cl ions. The open circles represent data points and the solid line represents a least squares fit of the spectrum.

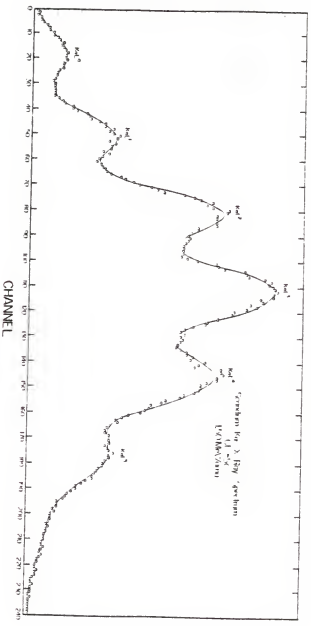
ARBITRARY UNITS
CHANNEL

As was discussed earlier, the average number of L-shell vacancies is proportional to the probability of L-shell ionization at very small impact parameters,

$$\langle \ell \rangle \propto P_L(0).$$

$P_L(0)$ may be obtained from the binary encounter approximation (BEA)[13] and the semiclassical approximation (SCA)[14] theories and, since there is no impact parameter development of the plane wave Born approximation theory (PWBA),[15] $P_L(0)$ may only be inferred from the PWBA theory. In all three theories, a simple projectile Z-dependence is expected for $P_L(0)$

$$P_L(0) \propto Z_1^2 G(V)$$

where Z, is the projectile nuclear charge and G(V) is a function of the scaled velocity, $V = V_{inc}/V_e$, where V_{inc} is the velocity of the incident projectile and V_e is the velocity of the electron in the target L-shell. This implies that $\langle \ell \rangle$ obeys the same Z_1 dependence (i.e. $\langle \ell \rangle \propto Z_1^2 G(V)$). The function, G(V), was tabulated for the BEA[13] and SCA theories[14] and can be calculated from a polynomial approximation for the PWBA theory.

A scaling function, f(V), to be compared to the function G(V), can then be obtained by simple algebra,

$$f(V) = \frac{\langle \ell \rangle}{KZ_1^2}.$$

This type of scaling has been shown in the past to be too strongly Z_1 dependent.[7,10]

Since single K-shell, multiple L-shell ionization is a small impact parameter effect for the L-shell, scaling functions for the PWBA, SCA, and BEA theories can be obtained by applying the ideas of increased orbital electron binding energy as used in the PWBA theory of Brandt and Lapicki.[16]

The comparisons of these scaling functions, f(V), with the functions predicted by the PWBA, BEA, and SCA theories will be discussed in Section III.

II. EXPERIMENTAL TECHNIQUE

The experiment was performed on the Kansas State University model EN 27 tandem Van de Graaff accelerator. Ions of C, N, O, F and Cl were accelerated to energies in the range of 0.50 MeV/amu to 2.75 MeV/amu. Protons were also accelerated to energies in the range of 1.00 MeV/amu to 4.00 MeV/amu. The beam currents were monitored by a current integrator using the thick scandium target as a beam stop. The resulting scandium x-rays were wavelength analyzed using a four-inch curved crystal spectrometer equipped with a LiF ($2d = 4.027$ Å) Johansson focusing crystal.

Figure 7 shows the properties of such a focusing crystal. First, the crystal must annealed and aligned along the proper axis. It is then machined (polished) to a circular cylinder form of radius 2R. Finally, the machined crystal is bent to a radius of R. The planes of the finished crystal are thus concentric with radius 2R about center O (see figure 7) so that segments OB and OA are perpendicular to the crystal's planes and OA is a diameter of the focal circle. If a source is placed on the focal circle at S and a detector on the focal circle at D such that the arcs SO and OD are equal, then, from geometry, angle SBD and angle SAD will be equal. Since the angle of incidence and the angle of reflection must be equal, all four ϕ's in figure 7 are equal and exact focusing is achieved. The crystal used in this experiment was obtained commercially.

X-rays reflected from such a crystal will also constructively interfer in integral multiples according to the Bragg law of reflection, $n\lambda = 2d \sin \theta$, where λ is the wavelength of the x-rays, θ is the angle between the crystal planes and the incident parth, and d is the spacing of the crystal planes. All the spectra for this paper were obtained in first

Figure 7: Geometric view of the focusing properties of the Johansson curved crystal.

REFLECTIVE FOCUSING BY THE JOHANSSON METHOD

CRYSTAL IS FIRST MACHINED
TO A RADIUS OF 2R

MACHINED CRYSTAL BENT TO RADIUS R

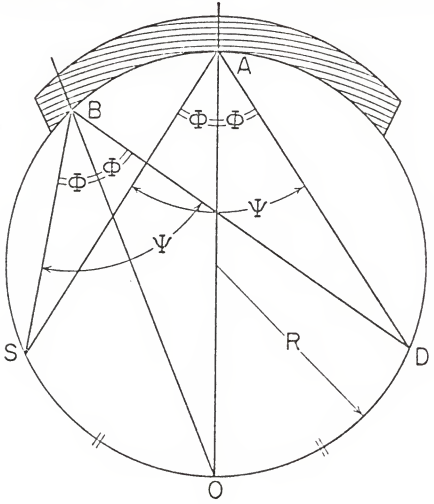

order; i.e. n = 1.

Measurements of the target x-rays were made with the four-inch curved crystal spectrometer placed at a 90° angle with respect to the beam axis as shown in figure 8. The scandium target was then placed in front of the spectrometer at a 45° angle with respect to the beam axis. The target x-rays entered the spectrometer and were Bragg reflected by the LiF curved crystal to a flow proportional counter which utilized a P10 gas mixture (10% methane and 90% argon) and a thin ($\sim$ 5000 Å) polypropalene window. The spectrometer was so designed that the target (source) and the proportional counter (detector) are always on the focal circle for all desired reflecting angles of this experiment. Scanning through the desired angles was achieved through use of a spectrometer stepping motor controlled by an on-line PDP-15 computer. The number of x-rays for a given amount of micro-Coulombs of integrated current at each angular setting of the crystal and detector was recorded until an entire scan of angles was achieved. Each spectrum so taken was repeated at least once to improve statistics. In this manner, the statistical errors were reduced to values of much less than 5%. Other errors, such as reproducibility errors and errors due to ignoring the L-shell vacancy dependence of the fluorescence yields, were found to be less than or on the order of 10%. The error bars in figure 15 and figure 18 are selected representatives of the magnitudes of the errors involved in this experiment. Figure 9 is a block diagram of the electronics.

Figure 8: A diagram of the target chamber used for this experiment.

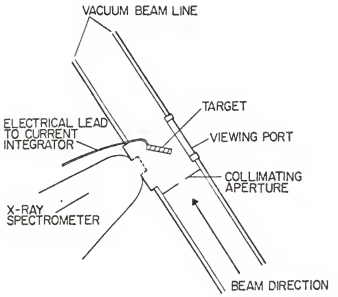
VACUUM BEAM LINE
TARGET
ELECTRICAL LEAD TO CURRENT INTEGRATOR
VIEWING PORT
COLLIMATING APERTURE
X-RAY SPECTROMETER
BEAM DIRECTION

Figure 9: Block diagram of electronics used in this experiment. The arrows indicate pulse direction.

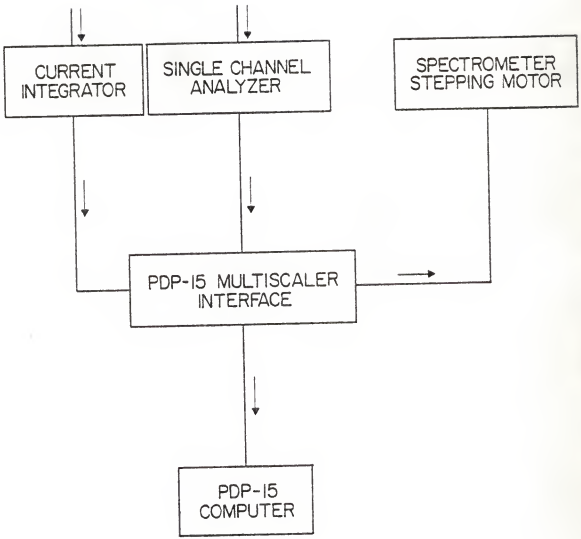
CURRENT INTEGRATOR
SINGLE CHANNEL ANALYZER
SPECTROMETER STEPPING MOTOR
PDP-15 MULTISCALER INTERFACE
PDP-15 COMPUTER

III. DISCUSSION

The relative satellite intensities, found in Table I, were used to calculate the average number of L-shell vacancies using the definition of $<\ell>$,

$$<\ell> \equiv \frac{\sum_n nI_n}{\sum_n I_n} .$$

I_n is the relative satellite intensity of the n^{th} satellite. The relative intensities in Table I were obtained, for the most part, by a least squares fit of the spectra. The relative intensities for oxygen, $Z_1 = 8$, at 0.50 MeV/amu and 1.00 MeV/amu, shown in parenthesis, were hand calculated.

Table II shows the values of $<\ell>$ calculated from the relative satellite intensities given in Table I. The values of $<\ell>$ are seen to increase with increasing projectile charge, Z_1, at a given projectile energy. The values of $<\ell>$ for C, N, O and F projectiles are seen to increase with increasing projectile energies up to a peak at approximately 1.50 MeV/amu and then are seen to decrease with increasing projectile energies. The values of $<\ell>$ for proton bombardment appear to be over the peak since they are seen to decrease with increasing energy. However, the values of $<\ell>$ for Cl bombardment are seen to increase with increasing projectile energy.

The nature of these values of $<\ell>$ as a function of the scaled velocity, $V = V_{inc}/V_e$, where V_{inc} and V_e were defined in section I, is shown plotted in figure 10. The Br data was taken from Jamison et al.[17] and the He data was taken from Kauffman et al.[8] Since a "universal" scaling was desired, an attempt to eliminate the projectile Z effect was tried. This simple $1/Z_1^2$ scaling, shown plotted in figure 11, was seen to be too strongly Z_1 dependent.

Figure 10: $\langle \ell \rangle$ versus V for Sc KL^n satellite data. The He data was taken from Kauffman et al. and the Br data was taken from Jamison et al. The lines are to guide the eye.

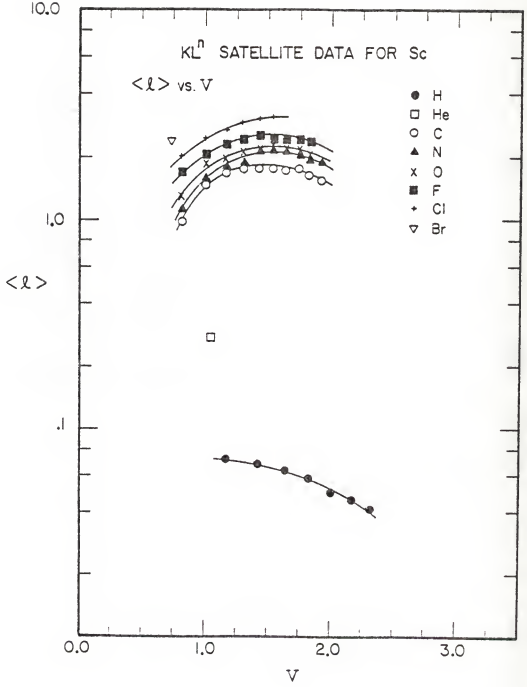
KL^n SATELLITE DATA FOR Sc
<ℓ> vs. V
H
He
C
N
O
F
Cl
Br
10.0
1.0
.1
<ℓ>
0.0
1.0
2.0
3.0
V

Figure 11: $\langle \ell \rangle / Z_1^2$ versus V for Sc KL^n satellite data. The He data was taken from Kauffman et al. and the Br data was taken from Jamison et al. The lines are to guide the eye.

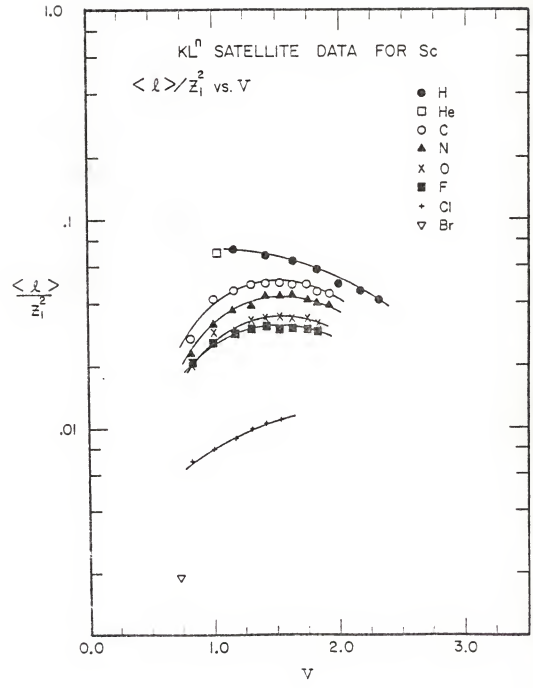
KL^n SATELLITE DATA FOR Sc
< ℓ >/Z_1^2 vs. V
H
He
C
N
O
F
Cl
Br
1.0
.1
.01
< ℓ >/Z_1^2
0.0
1.0
2.0
3.0
V

In anticipation of correcting the simple $1/Z_1^2$ scaling, Schmiedekamp et al.[11] applied the ideas of increased binding of Brandt and Lapicki.[16] The increased binding energy of the L-shell, U_L', in terms of the actual binding energy of the L-shell of the target, U_L, is given by

$$U_L' = \varepsilon U_L$$

where the binding correction, ε, is greater than unity. Several authors[16,18,19] have suggested using the form $\varepsilon = 1 + (2Z_1/Z_{2L}\zeta_L)g$ for the binding correction, where $Z_{2L} = Z_2 - 4.15$, ζ_L is given by $4U_L/\{Z_{2L}^2(13.6)\}$, and g is a velocity dependent correction term being totally independent of Z_1. The expression, while predicting a linear dependence on Z_1, does not extrapolate properly to the united atom limit.

Schmiedekamp et al.[11] suggested using the expression $\varepsilon = 1 + (aZ_1 + bZ_1^2)g(v)$, where g(v) is equation 19 of reference 16 and a and b are fitting parameters. Utilizing this expression in the BEA form of the projectile scaling to be discussed later in this section, Schmiedekamp et al.[11] obtained results which, for the lighter projectiles, were in excellent agreement with the ionization curve for Ar predicted by the PWBA theory. In an attempt to apply this scaling directly to the data for Sc, the parameters, a and b, from the expression for the binding correction and the parameter, K, from the BEA scaling were scaled from those for an Ar target to those for a Sc target. The expected values for the parameters, along with the results of the scaling of the Sc data, are shown in figure 12. Only the lighter projectile data were plotted since, as was discovered by Schmiedekamp et al.[11], the scaling was not expected to work well for the relatively heavier projectiles. The ionization curve for Sc predicted by the PWBA theory yields the same basic trend as the plotted data. However, the PWBA theoretical

Figure 12: Sc KL^n satellite data plotted using the BEA projectile scaling. The parameters ε and K were scaled from the values for Ar as shown.

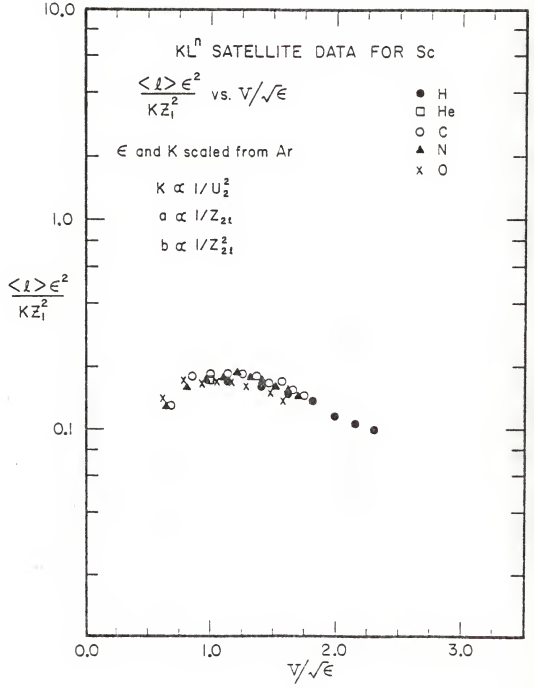
KL^n SATELLITE DATA FOR Sc
<ℓ>ε²/KZ₁² vs. V/√ε
ε and K scaled from Ar
K ∝ 1/U₂²
a ∝ 1/Z₂ₜ
b ∝ 1/Z₂ₜ²
H
He
C
N
O
10.0
1.0
0.1
0.0
1.0
2.0
3.0
V/√ε

ionization curve peaks at lower scaled velocities and has a lower magnitude by a factory of approximately two.

The idea of increased binding leads to two forms of the projectile scaling laws corresponding to the theories involved. In the PWBA and SCA theories, a function of the form

$$f(V/\varepsilon) = \frac{<\ell>\varepsilon}{KZ_1^2}$$

can be derived (see appendix) and compared to the BEA or PWBA ionization probability function. Figure 13 shows the results of the PWBA scaling (the data) in comparison with the BEA and PWBA ionization probability functions (the solid curves). The agreement for the heavier projectiles is bad while, for the lighter projectiles, the agreement improved. The final values for the fitting parameters a, b, and K are given in figure 13.

In the BEA theory, a function of the form

$$f(V\sqrt{\varepsilon}) = \frac{<\ell>\varepsilon^2}{KZ_1^2}$$

can be obtained (see appendix) and compared to the BEA or PWBA ionization probability function. Figure 14 shows the results of the BEA scaling (the data) in comparison with the BEA and PWBA ionization probability functions (the solid curves). As can be seen, the BEA scaling gives much better agreement than the PWBA scaling and, in comparison to either the BEA or the PWBA ionization probability function, gives excellent agreement for $Z_1/Z_2 \lesssim 0.4$. The agreement is also satisfactory for $0.4 \lesssim Z_1/Z_2 \lesssim 1.0$ with scaled velocities, $V \gtrsim 1.0$. For projectiles heavier than the scandium target, little or no agreement occurs with either the BEA or PWBA ionization function. The values of the fitting parameters a, b, and K are given in figure 14.

Figure 13: Sc KL^n satellite data plotted using the PWBA projectile scaling. In the upper plot, data is compared to the BEA ionization probability function (solid line). In the lower plot, data is compared to the PWBA ionization probability function (solid Line). The values of the fitting parameters are given in the figure.

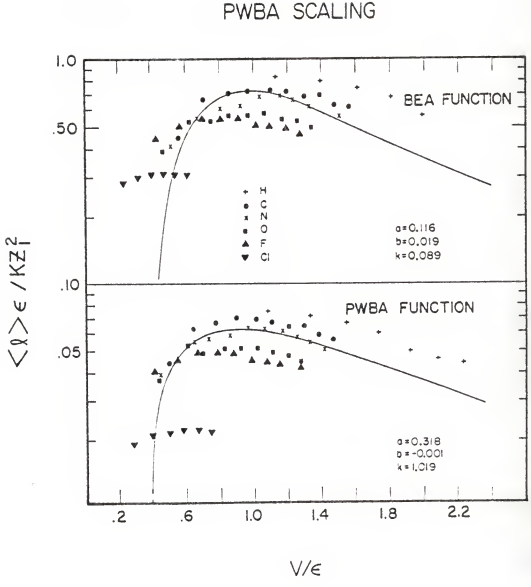
PWBA SCALING
BEA FUNCTION
a=0.116
b=0.019
k=0.089
PWBA FUNCTION
a=0.318
b=-0.001
k=1.019
H
C
N
O
F
Cl
1.0
.50
.10
.05
.2
.6
1.0
1.4
1.8
2.2
V/ϵ

Figure 14: Sc KL^n satellite data plotted using the BEA projectile scaling. In the upper plot, data is compared to the BEA ionization probability function (solid line). In the lower plot, data is compared to the PWBA ionization probability function. The values of the fitting parameters are given in the figure.

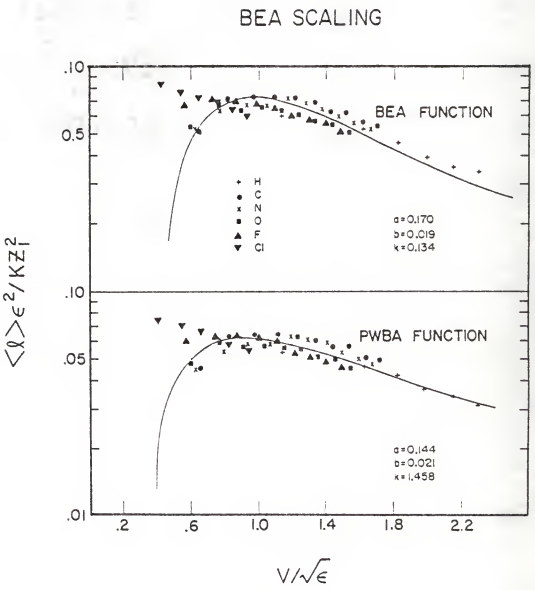
BEA SCALING
BEA FUNCTION
PWBA FUNCTION
H
O
N
O
F
Cl
a=0.170
b=0.019
k=0.134
a=0.144
b=0.021
k=1.458
.10
0.5
.10
.05
.01
.2
.6
1.0
1.4
1.8
2.2
$\langle \ell \rangle \epsilon^2 / KZ_1^2$
$V/\sqrt{\epsilon}$

With hopes of obtaining better agreement, the SCA ionization probability function was compared to the BEA scaling. The BEA scaling, although not the scaling predicted by the SCA theory, was chosen over the PWBA scaling since the BEA scaling produced superior agreement to either ionization probability function. Figure 15 shows the results of the BEA scaling compared to the SCA ionization probability function. Good agreement was extended to $Z_1/Z_2 \lesssim 0.8$ while, for $0.8 \lesssim Z_1/Z_2 \lesssim 1.0$, good agreement still occurs with scaled velocities of less than unity. Since little or no improvement of the latter range was achieved, the data was refitted omitting the chlorine data. The values for the fitting parameters a, b, and K are shown in figure 15.

In Table II, the values of the binding correction, ε, are given. The binding correction is seen to increase with increasing projectile charge, Z, at a given energy and to decrease with increasing energies for all projectiles.

Watson et al.[12] suggested using a scaling of the form

$$\bar{P}_L \frac{Z_2^{2.836}}{Z_1^2} = f(V),$$

where Z_2 is the target charge, Z_1 is the projectile charge, $\bar{P}_L$ is the average L-shell ionization probability, and f(V) is a "universal" velocity function of the scaled velocity, V. Figure 16 shows the data from the present work compared to the "universal" velocity function of Watson et al.[12] As can be seen from the figure, this scaling gave excellent agreement for the proton data, but the agreement deteriorated with increasing projectile charge, Z_1.

Figure 15: Sc KL^n satellite data plotted using the BEA projectile scaling and compared to the SCA ionization probabilty function. In the upper plot, the shown fitting parameters resulted from including the Cl data in the fit. In the lower plot, the shown fitting parameters resulted from excluding the Cl from the fit.

SCA FUNCTION

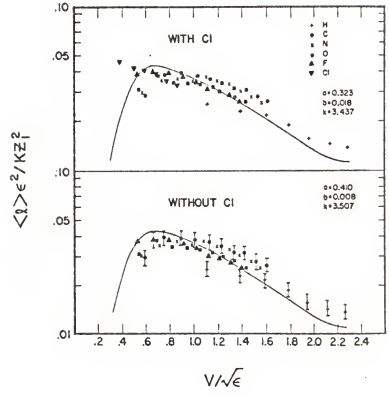

Figure 16: Sc KL^n satellite data plotted using the low projectile Z scaling of Watson et al. in comparison to a "universal" velocity function (solid line).

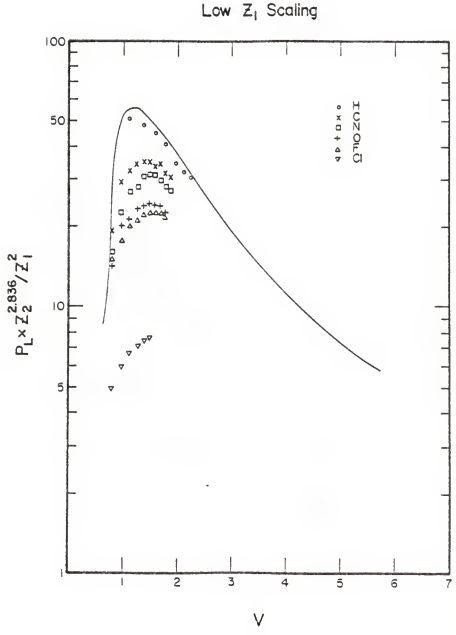
Low Z_1 Scaling
$P_L \times Z_2^{2.836}/Z_1^2$
V
100
50
10
5
1
1
2
3
4
5
6
7
HOUSTON

IV. CONCLUSION

The systematics of single K-shell, multiple L-shell ionization in ion-atom collisions over a large range of projectile Z and projectile energies have been extended from Ar gas targets to solid Sc targets. The results were used to test two recent semi-empirical "universal" scaling laws for predicting the distribution of Kα x-ray satellites in ion-atom collisions.

For light projectiles, the low Z scaling of $<\ell>$ by Watson et al.[12] gave good agreement over a fair range of scaled velocities. For heavier projectiles, $Z_1/Z_2 \gtrsim 0.2$, large deviations from the "universal" velocity function were found. This was expected from the results of Watson et al.[12] who suggested this scaling only for $Z_1/Z_2 << 1$.

The PWBA scaling gave poor agreement with both the PWBA and the BEA ionization probability functions.

For projectiles that satisfied $Z_1/Z_2 \lesssim 0.4$, the BEA scaling gave excellent agreement with both the BEA and the PWBA ionization probability functions. For projectiles that simultaneously satisfied $0.4 \lesssim Z_1/Z_2 \lesssim 1.0$ and $V \gtrsim 1.0$, good agreement was obtained. Using the SCA ionization probability function for comparison, excellent agreement was achieved over a larger projectile range, $Z_1/Z_2 \lesssim 0.8$, at all scaled velocities whereas the agreement remained unchanged for projectiles that simultaneously satisfied $0.8 \lesssim Z_1/Z_2 \lesssim 1.0$ and $V \gtrsim 1.0$. In all cases for the BEA scaling, poor agreement occurred for heavy projectiles, $Z_1/Z_2 > 1.0$.

It has been suggested that the areas of poor agreement may be attributed in part to partial screening of the target L-shell from the projectile nucleus by the projectile L-shell electrons. The effective projectile charge seen by the target would then be less than Z_1. If taken into account, this

Figure 17: <r> for projectile and target K-shells and L-shells. The arrows indicate projectiles for which data was available. The solid line is the value of <r> for the target Sc.

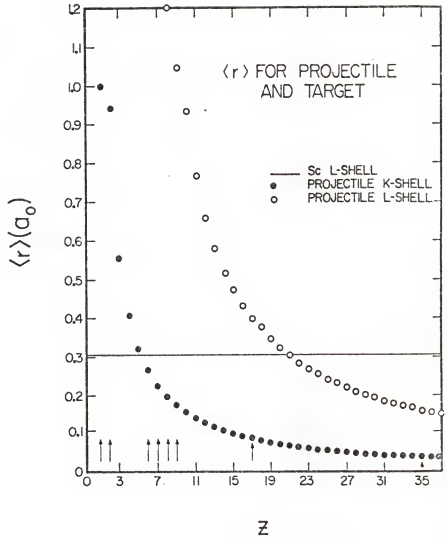
⟨r⟩ FOR PROJECTILE AND TARGET
Sc L-SHELL
PROJECTILE K-SHELL
PROJECTILE L-SHELL
⟨r⟩(a0)
Z
0
0.1
0.2
0.3
0.4
0.5
0.6
0.7
0.8
0.9
1.0
1.1
1.2
3
7
11
15
19
23
27
31
35

The results of scaling simply the parameters a and b in the expression for the binding correction and not scaling the magnitude parameter K are compared, in figure 18, to the SCA ionization probability function. The data was taken from the paper by Kauffman et al.[8] The parameters a and b were scaled for the various targets using the above suggestion from the values of a and b given in the lower plot of figure 15.

In conclusion, it can be seen that the BEA scaling when compared to the SCA ionization probability function yields the best agreement over the widest range of projectiles and scaled velocities. The scaling of the binding correction ε to various targets appeared to be an adequate scaling for the few cases tested. However, before any conclusive statement concerning this particular form of target scaling can be made, many more cases must be tested.

Figure 18: Oxygen induced KL^n satellite data plotted using the BEA projectile and suggested target scaling. The data is compared to the SCA ionization probability function.

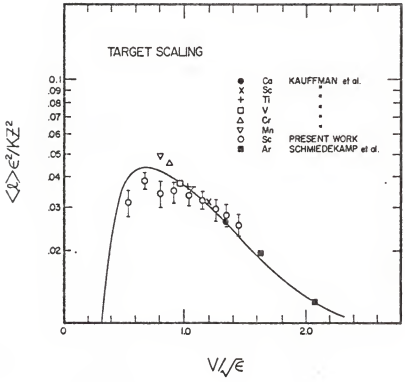
TARGET SCALING
Ca
Sc
Ti
V
Cr
Mn
Fe
Ni
Cu
Zn
Ga
Ge
As
Se
Br
Kr
KAUFFMAN et al.
PRESENT WORK
SCHMIEDEKAMP et al.
0.1
.09
.08
.07
.06
.05
.04
.03
.02
0
1.0
2.0
$\langle \rho \rangle \epsilon^2/KZ^2$
$V/\sqrt{\epsilon}$

would decrease the effect of the $1/Z_1^2$ scaling and all subsequent scalings. The expectation values of the projectile K-shell and L-shell radii, <r>, in units of the Bohr radius, a_o, are plotted as a function of Z in figure 17. The arrows indicate projectiles for which Sc satellite data was available. The solid line is the expectation value of the radius for the L-shell of Sc. The values of <r> for the heavier projectiles, notably Cl and Br, are seen to be approximately equal to or less than the value of <r> for Sc.

Another process which was not considered in this thesis but may be of significance for heavier projectiles is electron transfer from the projectile to the target. This process would tend to decrease the observed value of the average number of L-shell vacancies, <ℓ>, and thus, when taken into consideration in the calculations, would raise the value of <ℓ> in the simple $1/Z_1^2$ scaling and all subsequent scalings.

It must be remembered that all effects of vacancy rearrangement and vacancy-dependent fluorescence yields were ignored.

A possible method of extending this scaling to various other targets is suggested in this thesis. In section III, the parameters a and b were scaled from the values for Ar[11] to the values expected for Sc. The form of scaling used for the parameter was obtained by comparing the form of the binding correction used in this thesis to the form of the binding correction suggested in reference 16 and comparing like powers of the projectile charge Z_1. The parameter a was then assumed to be inversely proportional to $Z_{2L} = Z_2 - 4.15$ or $a \propto 1/Z_{2L}$. The form of scaling for b was obtained by assuming that the form of ε given in reference 16 was a truncated expansion in Z_1/Z_2 and then completing the comparison of like powers of Z_1. Thus, the form assumed for the parameter b was $b \propto 1/Z_{2L}^2$.

REFERENCES

1. P. Richard, I. L. Morgan, T. Furuta and D. Burch, Phys. Rev. Lett. 23, 1009 (1969).
2. D. Burch and P. Richard, Phys. Rev. Lett. 25, 983 (1970).
3. A. R. Knudson, K. J. Nagel, P. G. Burkhalter and K. L. Dunning, Phys. Rev. Lett. 26, 1149 (1971).
4. D. Burch, P. Richard and R. L. Blake, Phys. Rev. Lett. 26, 1355 (1971).
5. J. M. Hansteen, O. M. Johnsen and L. Kocbach, J. Phys. B 7, L271 (1974).
6. J. H. McGuire and P. Richard, Phys Rev. A 8, 1374 (1973).
7. F. Hopkins, D. O. Elliott, C. P. Bhalla and P. Richard, Phys. Rev. A 8, 2952 (1973).
8. R. L. Kauffman, J. H. McGuire, P. Richard and C. F. Moore, Phys. Rev. A 8, 1233 (1973).
9. T. K. Li, R. L. Watson and J. S. Hansen, Phys. Rev. A 8, 1258, (1973).
10. R. L. Kauffman, C. W. Woods, K. A. Jamison and P. Richard, Phys. Rev. A 11, 872 (1975).
11. C. Schmiedekamp, B. L. Doyle, T. J. Gray, R. K. Gardner, K. A. Jamison and P. Richard, Phys. Rev. A 18, 1892 (1978).
12. R. L. Watson, B. I. Sonobe, J. A. Demarest and A. Langenberg, Phys. Rev. A 19, 1529 (1979).
13. J. H. McGuire and K. Omidvar, Phys. Rev. A 10, 182 (1974).
14. J. M. Hansteen, O. M. Johnsen and L. Kocbach, At. Data and Nucl. Data Tables 15, 305 (1975).
15. B. H. Choi, E. Merzbacher and G. S. Khandelwal, At. Data 5, 291 (9173).
16. W. Brandt and G. Lapicki, Phys. Rev. A 10 474 (1974).

17. K. A. Jamison, C. W. Woods, R. L. Kauffman, and P. Richard, Phys. Rev. A 11, 505 (1975).

18. G. Basbas, W. Brandt and R. Laubert, Phys. Rev A 7, 983 (1973).

19. G. Lapicki and W. Losonsky, Phys. Rev A 15, 896 (1977).

Table I

Scandium
Relative Satellite Intensities

Z	$\frac{MeV}{amu}$	$K\alpha L^0$	$K\alpha L^1$	$K\alpha L^2$	$K\alpha L^3$	$K\alpha L^4$	$K\alpha L^5$	$K\alpha L^6$
1	1.00	0.9277	0.0723					
	1.50	0.9323	0.0677					
	2.00	0.9362	0.0638					
	2.50	0.9422	0.0578					
	3.00	0.9507	0.0493					
	3.50	0.9543	0.0457					
	4.00	0.9568	0.0432					
6	0.50	0.2946	0.4580	0.2162	0.0312			
	0.75	0.1756	0.3990	0.2554	0.0927	0.0773		
	1.00	0.1143	0.3505	0.3179	0.1676	0.0297		
	1.25	0.1100	0.3112	0.3342	0.1947	0.0499		
	1.50	0.1008	0.3048	0.3535	0.1873	0.0537		
	1.75	0.1096	0.2942	0.3525	0.1875	0.0562		
	2.00	0.1128	0.3119	0.3589	0.1719	0.0445		
	2.25	0.1167	0.3030	0.3277	0.1873	0.0654		
	2.50	0.1383	0.3448	0.3147	0.1597	0.0425		
	2.75	0.1568	0.3472	0.3129	0.1412	0.0420		
7	0.50	0.2389	0.4740	0.2066	0.0806			
	0.75	0.1318	0.3649	0.3018	0.2015			
	1.00	0.0992	0.2894	0.3560	0.1725	0.0729		
	1.25	0.0945	0.2547	0.3656	0.1938	0.0914		
	1.50	0.0623	0.2405	0.3251	0.2128	0.1583		
	1.75	0.0689	0.2351	0.3157	0.2259	0.1545		
	2.00	0.0682	0.2445	0.3026	0.2372	0.1476		
	2.25	0.0790	0.2498	0.3409	0.1920	0.1383		
	2.50	0.0926	0.2761	0.3372	0.1809	0.1133		
	2.75	0.1196	0.2660	0.3383	0.1711	0.1050		
8	0.50	(0.153)	(0.451)	(0.343)	(0.053)			
	0.75	0.1037	0.2820	0.3531	0.1932	0.0681		
	1.00	(0.062)	(0.252)	(0.415)	(0.235)	(0.036)		
	1.25	0.0707	0.2240	0.3433	0.2446	0.1174		
	1.50	0.0582	0.2110	0.3593	0.2499	0.1216		
	1.75	0.0551	0.2056	0.3554	0.2062	0.1777		
	2.00	0.0603	0.2200	0.3440	0.2456	0.1302		
	2.25	0.0576	0.2207	0.3312	0.2835	0.1070		
	2.50	0.0705	0.2434	0.3453	0.2454	0.0953		
9	0.50	0.1253	0.3162	0.3366	0.1615	0.0605		
	0.75	0.0715	0.2523	0.3378	0.2093	0.1291		
	1.00	0.0569	0.1955	0.3263	0.2059	0.2154		
	1.25	0.0769	0.1391	0.3417	0.2244	0.1498	0.0581	
	1.50	0.0723	0.1157	0.3692	0.2019	0.1363	0.1047	
	1.75	0.0622	0.1669	0.2928	0.2726	0.1460	0.0595	
	2.00	0.0547	0.1795	0.2784	0.2935	0.1313	0.0627	
	2.25	0.0567	0.1796	0.2840	0.2804	0.1366	0.0627	
	2.50	0.0564	0.1902	0.2859	0.2970	0.1281	0.0423	
17	0.50	0.0578	0.2710	0.3239	0.2787	0.0686		
	0.75	0.0353	0.1627	0.3264	0.3245	0.1179	0.0333	
	1.00	0.0315	0.1212	0.2635	0.3482	0.1666	0.0691	
	1.25	0.0283	0.0974	0.2035	0.3631	0.1942	0.1135	
	1.50	0.0292	0.0846	0.1960	0.3421	0.2329	0.0875	0.0278
	1.75	0.0337	0.0571	0.1850	0.3807	0.2102	0.1008	0.0325

Numbers in ( ) are hand calculated.

Table II

Binding-energy correction factors for Sc

			FWBA Scaling		BEA Scaling		SCA Curve BEA Scaling		
γ_1	$E\left(\frac{MeV}{amu}\right)$	$\langle 1 \rangle$	FWBA Curve	BEA Curve	FWBA Curve	BEA Curve	With CI	Without CI	United Atom Estimate
1	1.00	0.072	1.08	1.04	1.04	1.05	1.09	1.09	1.13
	1.50	0.048	1.07	1.03	1.04	1.04	1.07	1.09	1.13
	2.00	0.044	1.06	1.03	1.03	1.04	1.07	1.08	1.13
	2.50	0.058	1.06	1.02	1.03	1.03	1.06	1.07	1.13
	3.00	0.049	1.05	1.02	1.03	1.03	1.05	1.07	1.13
	3.50	0.046	1.05	1.02	1.02	1.03	1.05	1.06	1.13
	4.00	0.043	1.04	1.02	1.02	1.03	1.03	1.06	1.13
h	0.50	0.894	1.65	1.47	1.56	1.59	1.90	1.95	1.95
	0.75	1.487	1.55	1.40	1.48	1.51	1.77	1.81	1.95
	1.00	1.668	1.49	1.36	1.42	1.45	1.68	1.72	1.95
	1.25	1.763	1.45	1.33	1.38	1.41	1.62	1.65	1.95
	1.50	1.788	1.41	1.30	1.35	1.38	1.57	1.61	1.95
	1.75	1.787	1.39	1.28	1.33	1.35	1.53	1.57	1.95
	2.00	1.723	1.36	1.27	1.31	1.33	1.50	1.53	1.95
	2.25	1.782	1.34	1.25	1.30	1.31	1.48	1.51	1.95
	2.50	1.623	1.33	1.24	1.28	1.30	1.46	1.48	1.95
	2.75	1.564	1.31	1.23	1.27	1.29	1.44	1.46	1.95
	0.50	1.129	1.76	1.60	1.70	1.74	2.09	2.13	2.14
	0.75	1.573	1.64	1.51	1.60	1.63	1.93	1.96	2.14
	1.00	1.831	1.57	1.45	1.53	1.56	1.83	1.86	2.14
	1.25	1.933	1.52	1.41	1.48	1.51	1.75	1.78	2.14
	1.50	2.164	1.48	1.38	1.45	1.47	1.69	1.72	2.14
	1.75	2.162	1.45	1.46	1.42	1.44	1.65	1.67	2.14
	2.00	2.151	1.42	1.34	1.39	1.41	1.61	1.63	2.14
	2.25	2.061	1.40	1.32	1.37	1.39	1.58	1.60	2.14
	2.50	1.946	1.38	1.30	1.36	1.37	1.55	1.57	2.14
	2.75	1.876	1.37	1.29	1.34	1.36	1.53	1.55	2.14
g	0.50	1.296	1.86	1.74	1.86	1.90	2.30	2.32	2.33
	0.75	1.840	1.73	1.63	1.73	1.76	2.11	2.12	2.33
	1.00	1.931	1.65	1.56	1.65	1.68	1.98	1.99	2.33
	1.25	2.114	1.59	1.51	1.59	1.62	1.89	1.90	2.33
	1.50	2.164	1.55	1.47	1.55	1.57	1.83	1.84	2.33
	1.75	2.246	1.51	1.44	1.51	1.53	1.77	1.78	2.33
	2.00	2.165	1.48	1.41	1.48	1.50	1.73	1.74	2.33
	2.25	2.162	1.46	1.39	1.46	1.48	1.69	1.70	2.33
	2.50	2.052	1.44	1.37	1.44	1.45	1.66	1.67	2.33
	0.50	1.716	1.97	1.89	2.03	2.07	2.52	2.51	2.55
	0.75	2.072	1.82	1.76	1.88	1.91	2.30	2.28	2.55
	1.00	2.327	1.72	1.67	1.78	1.81	2.15	2.14	2.55
	1.25	2.435	1.66	1.61	1.71	1.74	2.05	2.04	2.55
	1.50	2.528	1.61	1.56	1.66	1.68	1.97	1.96	2.55
	1.75	2.452	1.57	1.53	1.61	1.64	1.90	1.89	2.55
	2.00	2.453	1.54	1.50	1.58	1.60	1.85	1.84	2.55
	2.25	2.449	1.51	1.47	1.55	1.57	1.81	1.80	2.55
	2.50	2.377	1.49	1.45	1.52	1.54	1.77	1.76	2.55
	0.50	2.029	2.79	3.57	3.94	3.94	4.74	--	4.88
	0.75	2.627	2.53	3.18	3.50	3.50	4.19	--	4.88
	1.00	2.704	2.35	2.94	3.22	3.22	3.83	--	4.88
	1.25	2.938	2.23	2.76	3.02	3.02	3.57	--	4.88
	1.50	3.038	2.14	2.63	2.87	2.86	3.38	--	4.88
	1.75	3.109	2.06	2.52	2.74	2.74	3.22	--	4.88

APPENDIX

The form of the PWBA projectile scaling can be obtained by substituting the increased binding energy $U_L' = \varepsilon U_L$ for the binding energy of the L-shell used in the calculations of reference 16.

Thus, the minimum momentum transfer for ionization of the L-shell including increased binding, $\hbar q_{0L}'$, is given by

$$\hbar q_{0L}' = \frac{2(U_L'/V_1)}{1 + (1 - U_L'/E_1)^{\frac{1}{2}}}. \tag{1}$$

Assuming the particle energy, $E_1 = \frac{1}{2}mV_1^2$, to be large compared to the binding energy U_L', $\hbar q_{0L}'$ may be approximated by

$$\hbar q_{0L}' \approx U_L'/V_1. \tag{2}$$

Substituting for U_L', $\hbar q_0'$ may be obtained in terms of the minimum momentum transfer without increased binding,

$$\hbar q_{0L}' = \frac{\varepsilon U_L}{V_1} = \varepsilon(\hbar q_{0L}). \tag{3}$$

At this point, a dimensionless quantity ξ_L' is defined,

$$\xi_L' = \frac{2}{q_{0L} a_{2L}} \tag{4}$$

where $a_{2L} = 4a_o/Z_{2L}$, a_o is the Bohr radius, and $Z_{2L} = Z_2 - 4.15$. Eliminating a_{2L} and q_{0L} from equation (4) yields

$$\xi_L' = \frac{\hbar V_1 Z_{2L}}{2U_L' a_o} \tag{5}$$

or, in terms of the dimensionless quantity with no increased binding ξ_L,

$$\xi_L' = \frac{1}{\varepsilon}\frac{\hbar V_1 Z_{2L}}{2U_L a_o} = \xi_L/\varepsilon. \tag{6}$$

ξ_L is a form of the scaled velocity $V = v_{inc}/v_e$ where v_{inc} and v_e are defined in section I.

Another dimensionless quantity Θ_L' is introduced,

$$\Theta_L' = \frac{4U_L'}{13.6Z_{2L}^2}. \tag{7}$$

This quantity also may be expressed in terms of the quantity without increased binding Θ_L as

$$\Theta_L' = \frac{4\varepsilon U_L}{13.6\ Z_{2L}^2} = \varepsilon\Theta_L \tag{8}$$

The ionization cross section may then be expressed in terms of ξ_L' and Θ_L by

$$\sigma_L = \frac{k_1 Z_1^2}{\Theta_L'} F_L(\xi_L') \tag{9}$$

where k_1 is a proportionality constant and $F_L(\xi_L')$ is a tabulated velocity function.[15]

Now $\langle \ell \rangle \propto P_L(0) \propto \sigma_L$, so an expression for $\langle \ell \rangle$ may be written,

$$\langle \ell \rangle = \frac{k_2 Z_1^2}{\Theta_L'} F_L(\xi_L') \tag{10}$$

where $\langle \ell \rangle$ is the average number of L-shell vacancies, k_2 is a proportionality constant and $F_L(\xi_L')$ may be approximated by a polynomial.[15]

Substitution of equation (6) and (8) into equation (10) yields

$$\frac{\langle \ell \rangle \varepsilon \Theta_L}{k_2 Z_1^2} = F_L(\xi_L/\varepsilon). \tag{11}$$

Replacing ξ_L with the scaled velocity V and absorbing Θ_L into the constant yields, for a given target, the form of the PWBA projectile scaling used in this thesis,

$$\frac{<\ell>\varepsilon}{KZ_1^2} = G(V/\varepsilon) \tag{12}$$

where $G(V/\varepsilon)$ is a new polynomial approximation to account for replacing ξ_L with V.

In the SCA theory including increased binding energy, the ionization probability for the L-shell I_L can be found from the tabulated generalized ionization probability function,[14] as

$$I_L = \frac{1}{Z_{2L}^2 \Theta_L'} f(X_L') \tag{13}$$

where

$$\Theta_L' = \frac{4U_L'}{13.6\ Z_{2L}^2}. \tag{14}$$

Again, Θ_L' may be written in terms of the quantity without increased binding,

$$\Theta_L' = \frac{4\varepsilon U_L}{13.6\ Z_{2L}^2} = \varepsilon\Theta_L. \tag{15}$$

The agrument of the generalized ionization probability function, X_L', is given by

$$X_L' = \frac{Z_{2L}\Theta_L'}{2\sqrt{E_1}} \tag{16}$$

where E_1, is the magnitude of the projectile energy in MeV. X_L' is a form of the inverse of the scaled velocity V. Substitution of equation (15) into equation (16) yields

$$X_L' = \frac{Z_{2L}\varepsilon\Theta_L}{2\sqrt{E_1}} = \varepsilon X_L'. \tag{17}$$

Thus, the ionization probability may be written as

$$I_L = \frac{k_1 Z_1^2}{\varepsilon\Theta_L} f(\varepsilon X_L) \tag{18}$$

where k_1 is a proportionality constant. Now $\langle \ell \rangle \propto P_L(0) = I_L$, so an expression for $\langle \ell \rangle$ may be written,

$$\langle \ell \rangle = \frac{k_2 Z_1^2}{\varepsilon\Theta_L} f(\varepsilon X_L) \tag{19}$$

where k_2 is a proportionality constant. But εX_L is proportional to ε/V so equation (19) becomes

$$\frac{\langle \ell \rangle \varepsilon}{K Z_1^2} = G(V/\varepsilon) \tag{20}$$

where K is a proportionality constant and $G(V/\varepsilon)$ is the appropriate form of $f(\varepsilon X_L)$.

It might be noted that this form of the projectile scaling is the same as the form obtained from the PWBA theory.

BEA Scaling

To obtain the form of the BEA projectile scaling, the increased binding energy U_L' was substituted for the binding energy U_L in the expression for the ionization cross section,

$$\sigma_L = \frac{k_1 Z_1^2}{(U_L')^2} G(V'). \tag{21}$$

$G(V')$ is a tabulated velocity function[13] and k_1 is a proportionality constant.

The scaled velocity V' is given by

$$V' = \sqrt{Em_e/MU_L'} = V/\sqrt{\varepsilon} \tag{22}$$

where E is the projectile energy, M is the projectile mass, m_e is the mass of an electron, and $U_L' = \varepsilon U_L$ is the increased binding energy.

Substituting equation (22) into equation (21) yields

$$\sigma_L = \frac{k_2 Z_1^2}{\varepsilon^2} G(V/\sqrt{\varepsilon}) \tag{23}$$

where U_L^2 has been absorbed by the proportionality constant k_2.

Now $\langle \ell \rangle \propto P_L(0) \propto \sigma_L$, so an expression for $\langle \ell \rangle$ may be written,

$$\langle \ell \rangle = \frac{KZ_1^2}{\varepsilon^2} G(V/\varepsilon) \tag{24}$$

or rearranging

$$\frac{\langle \ell \rangle \varepsilon^2}{KZ_1^2} = G(V/\varepsilon) \tag{25}$$

which is the form of the BEA projectile scaling used in this thesis.

A TEST OF MULTIPLE IONIZATION SCALING IN Sc

by

Joal J. Newcomb

B.S., Southwestern Oklahoma State University, 1976

AN ABSTRACT OF A MASTER'S THESIS

submitted in partial fulfillment of the

requirements for the degree

MASTER OF SCIENCE

Department of Physics

KANSAS STATE UNIVERSITY

Manhattan, Kansas

1979

ABSTRACT

A recent study of the projectile Z_1 and velocity dependence of single K-shell, multiple L-shell vacancy production in free atomic targets of Ar revealed a universal scaling of $<\ell>(=\sum_{\ell=0}^{7}\ell I_\ell / \sum_{\ell=0}^{7} I_\ell$ where I_ℓ is the measured intensity of the $K\alpha L^\ell$ satellite peak) based on an increased binding effect. In this thesis, scandium Kα x-ray satellites produced by ion-atom collisions were examined in high resolution using a 4" curved crystal spectrometer. Ions of H, C, N, O, F and Cl with energies in the range of 0.5 to 4.0 MeV/amu were used to investigate the scaling in solid scandium targets. The binary encounter approximation (BEA) scaling using either plane wave Born approximation (PWBA) or BEA ionization functions fit the data very well. An extension of the analysis was made in this thesis by comparing the date with the semiclassical approximation (SCA) ionization function. Other researchers have also proposed a scaling law for target K x-ray spectra applicable for light ions. Agreement between the data and the scaling prediction is good only for H projectiles. A method of scaling to different targets is also suggested in the present work.